I_f and SR Ca^{2+} release both contribute to pacemaker activity in canine sinoatrial node cells

Zhan Gao[1,a], **Biyi Chen**[1,a], **Mei-ling A. Joiner**[1], **Yuejin Wu**[1], **Xiaoqun Guan**[1], **Olha M. Koval**[1], **Ashok K. Chaudhary**[1], **Shane R. Cunha**[1], **Peter J. Mohler**[1,2], **James B. Martins**[1], **Long-Sheng Song**[1], and **Mark E. Anderson**[1,2,*]

[1]Department of Internal Medicine, University of Iowa, Iowa City, IA 52242, USA

[2]Departments of Molecular Physiology and Biophysics, University of Iowa, Iowa City, IA 52242, USA

Abstract

Increasing evidence suggests that cardiac pacemaking is the result of two sinoatrial node (SAN) cell mechanisms: a 'voltage clock' and a Ca^{2+} dependent process, or 'Ca^{2+} clock.' The voltage clock initiates action potentials (APs) by SAN cell membrane potential depolarization from inward currents, of which the pacemaker current (I_f) is thought to be particularly important. A Ca^{2+} dependent process triggers APs when sarcoplasmic reticulum (SR) Ca^{2+} release activates inward current carried by the forward mode of the electrogenic Na^+/Ca^{2+} exchanger (NCX). However, these mechanisms have mostly been defined in rodents or rabbits, but are unexplored in single SAN cells from larger animals. Here, we used patch-clamp and confocal microscope techniques to explore the roles of the voltage and Ca^{2+} clock mechanisms in canine SAN pacemaker cells. We found that ZD7288, a selective I_f antagonist, significantly reduced basal automaticity and induced irregular, arrhythmia-like activity in canine SAN cells. In addition, ZD7288 impaired but did not eliminate the SAN cell rate acceleration by isoproterenol. In contrast, ryanodine significantly reduced the SAN cell acceleration by isoproterenol, while ryanodine reduction of basal automaticity was modest (~14%) and did not reach statistical significance. Importantly, pretreatment with ryanodine eliminated SR Ca^{2+} release, but did not affect basal or isoproterenol-enhanced I_f. Taken together, these results indicate that voltage and Ca^{2+} dependent automaticity mechanisms coexist in canine SAN cells, and suggest I_f and SR Ca^{2+} release cooperate to determine baseline and catecholamine-dependent automaticity in isolated dog SAN cells.

Keywords

sinoatrial node cells; action potentials; funny current; sarcoplasmic reticulum; pacemaker

Introduction

The sinoatrial node (SAN) cardiac pacemaker was discovered a hundred years ago and has been extensively studied. [1] However, the pacemaking mechanisms of SAN cells remain unresolved and controversial. [2-3] Classically, ionic currents in the membrane of the

pacemaker cells are considered to support a 'voltage clock', in which the SAN cell ion channels coordinately orchestrate rhythmic action potentials (APs). Various ionic currents including the pacemaker current or funny current (I_f), L-type Ca^{2+} current ($I_{Ca.L}$), the delayed rectifier K^+ current (I_K) and the T-type Ca^{2+} current ($I_{Ca.T}$) may contribute to the voltage clock. [2] However, the I_f pacemaker current [4] is believed to provide decisive control over the voltage clock. I_f is conducted by a family of ion channel proteins, collectively known as hyperpolarization-activated cyclic nucleotide-gated ion channels (HCN). HCN contains four subtypes and HCN_4 is predominant in cardiac SAN cells. [5] Inward I_f mostly contributes to early phase 4 diastolic depolarization (DD) and increases in I_f during β adrenergic receptor stimulation steepen the DD rate leading to an increase in heart rate. [6]

There is a growing body of evidence, mostly derived from the SAN cells from small animals (i.e. mice, rats and rabbits), to support an I_f-independent, Ca^{2+}-dependent pacemaking mechanism referred to as a 'Ca^{2+} clock,' in which the intrinsic rhythmic local Ca^{2+} release from the sarcoplasmic reticulum (SR) drives SAN automaticity. SR Ca^{2+} release is thought to contribute to late DD by activating the forward mode of the electrogenic sarcolemmal Na^+-Ca^{2+} exchanger (NCX) to generate an inward current. [7-9] This Ca^{2+} dependent process is responsive to β adrenergic receptor stimulation that results in increased SR Ca^{2+} uptake and release.

The pacemaking mechanisms in single SAN cells from large animals remain unexplored. It is uncertain whether the voltage- and Ca^{2+}-dependent mechanisms co-exist in large animals, as appears to be the case in SAN cells isolated from rodents and rabbits. This knowledge gap is an obstacle to translating mechanisms learned in small animals to large animals, including humans. Recent studies using undisrupted canine SAN demonstrated that a Ca^{2+}-dependent process is likely to be important in larger animals. [10-11] In our study, we measured the contribution of I_f and SR Ca^{2+} release to basal and isoproterenol-stimulated SAN cells isolated from dogs. Our results show that voltage and Ca^{2+} clock mechanisms are operative in dog SAN cells, and support a concept that both mechanisms are required for physiological catecholamine-stimulated heart rate increases.

Material and Methods

Canine SAN cell isolation

Single SAN cells were isolated from canine heart based on a method used for mice. [12] Healthy adult mongrel dogs of either sex weighting 14-22 kg were included. This protocol was approved by the Animal Care and Use Review Board at The University of Iowa and conformed to all regulations for animal use including guidelines of American Physiology Society. Dogs were sedated with ketamine (5mg/kg, im) and acepromazine maleate (0.5mg/kg, im). Anesthesia was induced by slow i.v. administration of thiopental sodium (10mg/kg) followed by an α-chloralose (150mg/kg) bolus. After loss of consciousness and withdrawal reflexes the heart was quickly excised and put into cold Tyrode solution. The solution consists of (mM) 140 NaCl, 5.0 HEPES, 5.5 glucose, 5.4 KCl, 1.8 $CaCl_2$, 1.0 $MgCl_2$, pH adjusted to 7.4 with NaOH. The SAN region, delimited by the crista terminalis, atrial septum and orifice of superior vena cava, was dissected from heart. The SAN tissue was isolated from the immediate vicinity of the SAN artery, dissected into small chunks, and incubated in a 'low Ca^{2+}' solution at 37 °C. This solution contains (mM) 140 NaCl, 5.0 HEPES, 5.5 glucose, 5.4 KCl, 0.2 $CaCl_2$, 0.5 $MgCl_2$, 1.2 KH_2PO_4, 50 taurine and 1 mg/ml bovine serum albumin (BSA), with pH adjusted to 6.9 with NaOH. The SAN tissue was then digested in 10 ml of enzyme solution with collagenase type I (Worthington, Lakewood, NJ), elastase (Worthington, Lakewood, NJ), and protease type XIV (Sigma, St Louis, MO) in 'low Ca^{2+}' solution for about 30 min. The tissue was then transferred to 10 ml of Kraft-Brule medium containing (mM) 100 potassium glutamate, 5.0 HEPES, 20 glucose, 25 KCl, 10 potassium aspartate, 2.0 $MgSO_4$, 10

KH_2PO_4, 20 taurine, 5 creatine, 0.5 EGTA, and 1 mg/ml BSA, with pH adjusted to 7.2 with KOH. The tissue was gently agitated using a glass pipette for 5 mins. The dissociated cells were then stored at 4 °C and were used within 8 hours after isolation.

Electrophysiology

The cell suspension was placed in a chamber mounted on an inverted microscope. SAN cells were easily identified prior to voltage or current clamp studies by their typical morphology (spindle or spider shape), sustained rhythmic activity, and smaller size compared to atrial myocytes. Membrane ion channel currents and spontaneous APs were recorded using the perforated (amphotericin B) patch-clamp technique, all the experiments were performed at 36 ±1 °C, as previously reported. [12]

Spontaneous APs were recorded in Tyrode's solution with the pipette filled with (mM) 130 potassium aspartate, 10 NaCl, 10 HEPES, 0.04 $CaCl_2$, 2.0 MgATP, 7.0 phosphocreatine, 0.1 NaGTP, amphotericin B 240 μg/ml, with pH adjusted to 7.2 with KOH. Only the cells with stable and regular APs were included for the study.

I_f was recorded as described previously. [13-14] The currents were elicited with the command voltage steps applied for 2.0 s ranging from −120 mV to −40 mV in 10 mV increments from the holding potential of −35 mV. Patch pipettes were filled with intracellular solution, containing (mM): 120 potassium aspartate, 25 KCl, 4.0 $MgCl_2$, 10 EGTA, 4.0 KATP, 2.0 NaGTP, 2.0 phosphocreatine, 5.0 HEPES, 1.0 $CaCl_2$, and pH was adjusted to 7.2 with KOH. The extracellular solution contained (mM): 130 NaCl, 5.0 KCl, 2.0 $MgCl_2$, 1.8 $CaCl_2$, 5.0 HEPES, and pH was adjusted to 7.4 with NaOH. After the initial current recordings, 0.5 mM $BaCl_2$ was applied to eliminate the Ba^{2+}-sensitive component of K^+ current.

Immunofluorescence studies

Isolated canine SAN cells were gently washed with phosphate-buffered saline (PBS, pH 7.4) and immediately fixed in 2% paraformaldehyde for 20 min. Cells were blocked/permeabilized in PBS containing 0.075% Triton X-100, 2 mg/ml BSA and 3% fish gelatin, and incubated in HCN_4 primary antibody (Alomone Labs Ltd, Israel) overnight at 4 °C. Following PBS washes, cells were incubated in secondary antibody (Molecular Probes, Carlsbad, CA) for 2 hours at room temperature and mounted using Vectashield (Vector) and #1 coverslips. Images were collected on Zeiss 510 Meta confocal microscope (63 power oil 1.40 NA (Zeiss), pinhole equals 1.0 Airy Disc) using Carl Zeiss Imaging software.

Intracellular Ca^{2+} transients and sparks

Intracellular Ca^{2+} transients and sparks were observed using the confocal microscope, as described. [12,15] Briefly, the SAN cells were loaded with 5 μM Fluo-4 acetoxymethyl ester for 10 min, and then rested for 20 min for deesterification in normal Tyrode's solution. The cells were then placed on the recording chamber mounted on a confocal Ca^{2+} imaging system (LSM510, Carl Zeiss MicroImaging), the Ca^{2+} imaging was acquired by perfusing the cells with either normal Tyrode's solution or various drugs at 36±1 °C (Temperature Controller, TC2BIP, Cell MicroControls). Line scan mode was used at a speed of 1.92 ms per line and the scan lines were applied along the cell edge, because Ca^{2+} release occurs mostly in the SAN cell periphery. [16-17] Ca^{2+} transients and sparks were analyzed offline with IDL program (Research System Inc.)

Drugs

ZD7288 was purchased from Tocris Inc. (Ellisville, MI), ryanodine was purchased from Alexis Biochemicals (Plymouth Meeting, PA). All other chemicals were purchased from Sigma Co.

(St Louis, MO). Except isoproterenol, which was dissolved in water, all other chemicals were dissolved in dimethyl sulfoxide (DMSO) with stock solutions at the concentration of 10,000 times of the working solution. The stock solutions were aliquoted and stored at −20 °C. 0.01% DMSO was tested as the vehicle and showed no effect on ion channel currents and APs in SAN cells.

Data analysis

The data are presented as means ± the standard error of the mean (S.E.M, n=number of cells). The statistical significance was evaluated by using Student's *t* test or one-way ANOVA, as appropriate. Statistically significant differences were determined as P<0.05.

Results

1. APs in canine SAN cells

Canine SAN cells were easily identified by their typical morphology (spindle or spider shape) (Fig 1A), [13-14,18] HCN_4 expression (Fig 1B) and spontaneous APs (Fig 1C). Isolated SAN cells showed spontaneous APs that were initiated by a phase 4 DD (Fig 1C). The average spontaneous AP rate in isolated SAN cells was 115±3/min (n=85), which is similar to that observed in canine SAN tissue, [11] slightly higher than rates observed in isolated human SAN cells, [19] but slower than rates obtained in mouse, [12] rat, [20] or rabbit [21] SAN isolated cells. The maximum diastolic potential (MDP) was −56.8±1.0 mV (n=85), close to the results obtained in human [19] and small animal [14] preparations. Isoproterenol increased the pacemaker activity of the SAN cells in a concentration-dependent manner (Fig 1D). The IC_{50} for isoproterenol was 20.3 nM and the AP rate was increased by 80±8 % in the presence of 1 µM isoproterenol. These data show that canine SAN cells share several morphological and electrophysiological features with small animal SAN cells, but have a slower basal spontaneous AP rate that is more similar to humans than rodents or rabbits.

2. I_f inhibition reduced pacemaker activity and caused arrhythmia

We first sought to characterize the I_f currents in isolated canine SAN cells and to determine whether I_f plays a critical role in spontaneous SAN cell activity. Under our experimental conditions, the AP cycle length is approximately 500 ms, therefore we calculated I_f densities at 500 ms after the test potentials were applied. I_f was elicited by test potentials from −120 mV to − 40 mV from a holding potential of −35 mV in dog SAN cells. I_f was evident in response to test potentials relevant to DD (−50 - −70 mV) (Fig 2A). I_f was dramatically inhibited by 3 µM ZD7288 (Fig 2B), a selective I_f inhibitor, consistent with an earlier report. [22] In contrast, 3 µM ZD7288 did not affect peak L-type Ca^{2+} currents ($I_{Ca.L}$) (Supplementary Fig S1). I_f was significantly increased by isoproterenol (1 µM), consistent with traditional concepts that I_f participates in heart rate acceleration by β-adrenergic receptor stimulation (Fig 2C and D). In order that our data in dog are comparable to data reported in other species, we also measured the I_f at the end of the test pulses (2 s); the current density was 8.4±0.6 pA/pF (n=38) at −120 mV. it seemed that the I_f density is slightly higher than that obtained in isolated human SAN cells (~6 pA/pF), [23] but lower than I_f density from rabbit (10±4.8 pA/pF, n=23) [24] or mouse (18±2 pA/pF, n=23) SAN cells. [14] The relatively lower I_f densities in dog and human SAN cells may contribute to the slower heart rate in large animals. These data show that I_f is present in isolated dog SAN cells at a density that is characteristic of larger animals, but at a lower density than reported in SAN cells from smaller animals.

We used I_f antagonist drugs to study the contribution of I_f to the automaticity of canine SAN cells. The spontaneous rate of the SAN cells was reduced by 27±3% from 127±5 AP/min to 91±4 AP/min (n=13) in the presence of 3 µM ZD7288 (Fig 3A). Furthermore, the phase 4 DD was impaired, and the AP rate became irregular (Fig 3B). ZD7288 reduced the AP rate (Fig

3C), and tended to slow DD rates (Fig 3D), although the DD slowing effects of ZD7288 did not reach statistical significance (p=0.07) compared to basal conditions. ZD7288 resulted in a negative shift of MDP by about 3 mV (p=0.03, n=13) (Fig 3E), but did not significantly affect action potential amplitude (APA) (Fig 3F, p=0.06, n=13). The negative shift of MDP by I_f blocking suggested that I_f contributed to the maintenance of the physiologically depolarized membrane potential in dog SAN cells. The DD comprises of two components: an early linear component, and a later, nonlinear component. I_f currents are thought to contribute to the early linear part of DD. Consistent with previous studies in rabbit, [7,25] we found ZD7288 dramatically reduced the slope of early diastolic depolarization (EDD), but did not significantly affect AP take-off potentials (TOP) (Supplementary data Fig S3A-B), conforming I_f is specifically involved in early diastolic depolarization. These data showed that I_f significantly contributes to basal automaticity of isolated canine SAN cells, similar to reports in small animal SAN cells.

To examine whether inhibition of I_f would also affect AP rate acceleration by β-adrenergic receptor stimulation, we perfused SAN cells with 1 μM isoproterenol after pretreatment with ZD7288. Isoproterenol significantly increased SAN automaticity in the continuous presence of ZD7288 (P=0.03, compared to ZD7288 treatment in the absence of isoporterenol, n=6). However, the increase in SAN activity by isoproterenol after ZD7288 (36±5% increase, compared with ZD7288 treatment) was significantly (P=0.001) lower than that with isoproterenol alone (80±8%) (Fig 3C). We used two additional approaches to inhibit I_f: ivabradine (10 μM, n=4) and Cs^+ (3 mM, n=4). We found that both I_f antagonists produced similar effects to ZD7288 on SAN cells (data not shown). Taken together, our data suggest that I_f is an important component of SAN rate acceleration by β-adrenergic receptor stimulation. We interpret our findings that I_f antagonist drugs do not eliminate spontaneous automaticity or prevent rate increases in response to isoproterenol to suggest that other I_f - independent mechanisms also contribute to canine SAN cell physiology, consistent with recent studies of intact canine SAN tissue. [11]

3. The Ca^{2+} clock is important for physiological automaticity responses to isoproterenol

We measured intracellular Ca^{2+} and APs simultaneously in spontaneously active SAN cells using confocal microscopy and current-clamp mode. Consistent with previous reports in mouse and rabbit, [12,16] the representative images showed that most of the local intracellular Ca^{2+} release (LCR) was immediately prior to the global transients, suggesting LCR occurs in late diastole, during phase 4 DD (Fig 4A). Isoproterenol (1 μM) enhanced intracellular Ca^{2+} release (Fig 4B). The summary data showed that isoproterenol significantly increased the Ca^{2+} transient amplitude (Fig 4C) and the Ca^{2+} spark frequency, amplitude and duration (Fig 4D-F), but the width of the Ca^{2+} sparks was not significantly altered by isoproterenol (Fig 4G). These results are consistent with the concept that isoproterenol stimulates spontaneous SAN activity via enhancement of intracellular Ca^{2+} release. [26]

To test if local Ca^{2+} release is linked to the nonlinear diastolic depolarization phase. We calculated the time course of local Ca^{2+} release (LCR) and AP DD variance as described previously [7,9]. Fig 5A showed that LCR occurred during the nonlinear DD, and reached to the peak before the next AP upstroke. Furthermore, the time course of DD variance and that of LCR events are virtually superimposable, which is consistent with a study in rabbit SAN cells. [7,9] We also found the isoproterenol effects to decrease the spontaneous cycle length are linked to its effects on the LCR period (Fig 5B-C), although isoproterenol did not significantly alter the LCR size (Fig 5D). These results showed that LCR events correlate with beating rate.

To evaluate the functional role of the Ca^{2+} clock in the isolated SAN cells, we used ryanodine (2 μM) to inhibit the SR Ca^{2+} release. SAN cell automaticity slightly increased at the initial

phase of ryanodine treatment, and then gradually fell below control levels (Fig 6A). In the continuous presence of ryanodine, isoproterenol (1 μM) failed to significantly increase SAN pacemaking activity (Fig 6A-B). Ryanodine marginally reduced basal SAN automaticity (Fig 6C) by 14±4% from 126±7/min to 108±10/min (n=11, P=0.21) and non-significantly (P=0.24) decreased the rate of DDR (Fig 6D). A Ca^{2+} dependent process is thought to contribute to the late non-linear part of DD, [7] and consistent with previous studies in rabbit [7,25] we found ryanodine altered the late non-linear component, but not the early part of DD (Supplementary Fig S3C-D). While isoproterenol did increase SAN activity by 17.8 ± 5.9% (n=6) after pretreatment with ryanodine (P=0.052), the increase in SAN rate by isoproterenol in the presence of ryanodine treatment was significantly (P=0.002) less than with isoproterenol alone (Fig 6C). Ryanodine did not significantly alter MDP (Fig 6E) or APA (Fig 6F). We repeated this study with a higher ryanodine concentration (10 μM) and found similar results (data not shown). We interpret these data to mean that SR Ca^{2+} release is important for physiological automaticity increases by β-adrenergic receptor stimulation in canine SAN cells. Ryanodine did not prevent spontaneous activity in canine SAN cells, even though the global AP-induced Ca^{2+} transient and diastolic LCR were largely inhibited by 2 μM ryanodine, consistent with a previous study [27] and confirmed by confocal Ca^{2+} imaging (data not shown).

We next tested the possibility that the effects of ryanodine on SAN cell automaticity could result from alteration of I_f, suggesting that Ca^{2+} and voltage clock mechanisms were interrelated by a mutual dependence on I_f. We recorded I_f before and after 1 μM isoproterenol in the presence or absence of ryanodine pretreatment. For the pretreatment group, the SAN cells were perfused with 2 μM ryanodine for at least 20 minutes, to mirror the ryanodine exposure duration in our AP experiments (Fig 6). We found that I_f densities significantly and equivalently increased after application of isoproterenol, in the presence or absence of ryanodine (Fig 7). We also found ryanodine treatment did not significantly affect peak $I_{Ca.L}$ (Supplementary Fig S2), another inward current implicated in SAN function.[28] Taken together, these data show ryanodine did not affect $I_{Ca.L}$ or I_f in dog isolated SAN cells, supporting a concept that the Ca^{2+} and voltage clock mechanisms are not mutually dependent on I_f.

Discussion

Our results indicated that both voltage and SR Ca^{2+} release mechanisms are important for maintaining physiological activity of canine SAN cells. Although basal beating rates are very different from small to large animals, the pacemaker mechanisms in dog appears to be similar to those observed in rabbits, mice and rats. [2,9,29] In our view, the shared dependence of dog SAN cells on voltage and Ca^{2+} clock mechanisms suggests that studies from SAN cells and tissue in genetically modified mice are relevant to SAN biology in larger animals. However, it will be important to consider that expression levels of specific membrane ion channels and other Ca^{2+} cycling proteins vary across species, so that the relative contribution of particular ionic currents and Ca^{2+} signaling molecules may be different in different species.

Our study showed that HCN_4 was readily detected in the SAN cells but not in atrial cells, which is consistent with the results in mouse and other animals. [30] I_f was activated at membrane voltages in the DD range of canine SAN cells, and isoproterenol significantly increased I_f. The unique properties of I_f imply that it may play important roles in generation of pacemaker activity and modulation of heart rate by autonomic stimulation. [31] By using three different types of I_f antagonists, we confirmed that inhibition of I_f reduced basal pacemaking activity and blunted the response to isoproterenol. These results are in agreement with observations in humans and small animals. [23,32] Interestingly, our data showed that I_f blockers caused significant arrhythmia in single canine SAN cells, which resembled defects in sinus rate in patients with a familial HCN_4 mutations. [33-34] Remarkably, complete or near complete I_f

inhibition attenuated, but did not eliminate SAN rate increases by isoproterenol, indicating that I_f is not the only downstream target for fight or flight heart rate increases by catecholamines in canine SAN cells. Although it is formally possible that the tiny remnant currents after I_f inhibition contribute to rate increases after isoproterenol, we believe that our evidence points to the existence of an I_f -independent, Ca^{2+}-dependent mechanism that enables SAN automaticity increases with catecholamines.

SR Ca^{2+} release plays a central role in the Ca^{2+}-dependent modulation of SAN cells. Confocal Ca^{2+} imaging showed that the local Ca^{2+} release was present during late DD in canine SAN cells, and isoproterenol significantly increased DD SR Ca^{2+} release, suggesting that a Ca^{2+}-dependent process plays a critical role in pacemaking activity. In this study, the beating rate slightly increased at the beginning of superfusion of ryanodine, which is consistent with other observations, [11] and suggests that ryanodine initially increases SR Ca^{2+} release, and thus enhances inward NCX current to stimulate heart rate. The effects of a high concentration (> 1 μM) of ryanodine on SAN automaticity varies in different studies and the magnitude of SAN rate reduction ranges from no effect to complete elimination of automaticity. [26] We showed that ryanodine reduced basal pacemaker activity by around 14 %, which is similar to the observations in canine SAN tissue, in which ryanodine at 3 μM inhibited the beating rate by around 17%. [11] The discrepancy in the effects of ryanodine across various studies might result from several factors, such as species differences, experimental conditions, the quality of isolated cells and experimental preparations. Interestingly, the present study showed ryanodine only marginally reduced basal automaticity, but dramatically impaired the rate acceleration by isoproterenol. In agreement with our results, most studies in this field found ryanodine slightly decreased the automaticity at baseline (10%-40%), but strikingly attenuated the rate acceleration by β-adrenergic receptor stimulation (80-100%). [26] In our opinion, the mechanisms remain uncertain, but we speculate that many factors contribute to physiological pacemaking activity and to the chronotropic response to catecholamines in SAN cells, including I_f, other membrane ion channels and LCR events. We interpret the reduced chronotropic efficacy of isoproterenol after ryanodine to mean that SR Ca^{2+} release is critical for catecholamine-stimulated heart rate increases in canine SAN cells.

I_f density was not affected by ryanodine, before or after isoproterenol, indicating that the ryanodine actions on SAN automaticity did not result from actions on I_f, consistent with previous reports in rabbit and mouse SAN cells. [12,16] Our finding is different from one report, [35] in which isoproterenol failed to increase I_f in rabbit SAN cells at the presence of ryanodine. We don't know the reasons for the discrepancy, but guess these differences might result from the species or experimental conditions. We interpret the lack of effect of ryanodine on I_f to suggest that SR Ca^{2+} release is not critical for I_f in canine SAN.

Limitations

In this study we isolated SAN cells from the immediate vicinity of the SAN artery, but did not explicitly discriminate between central and peripheral SAN cells. Thus, our cells are likely a mixture from the SAN center and periphery. Although we found that the cells included in our study were similar in the basic properties we measured, it may be important in future studies to separate the SAN cells from different regions.

Supplementary Material

Refer to Web version on PubMed Central for supplementary material.

Acknowledgments

References

1. Dobrzynski H, Boyett MR, Anderson RH. New insights into pacemaker activity: promoting understanding of sick sinus syndrome. Circulation 2007;115(14):1921–32. [PubMed: 17420362]

2. Mangoni ME, Nargeot J. Genesis and regulation of the heart automaticity. Physiol Rev 2008;88(3): 919–82. [PubMed: 18626064]

3. Lakatta EG, Difrancesco D. What keeps us ticking: A funny current, a calcium clock, or both? J Mol Cell Cardiol. 2009

4. Baruscotti M, Barbuti A, Bucchi A. The cardiac pacemaker current. J Mol Cell Cardiol 2010;48(1): 55–64. [PubMed: 19591835]

5. Shi W, Wymore R, Yu H, Wu J, Wymore RT, Pan Z, et al. Distribution and prevalence of hyperpolarization-activated cation channel (HCN) mRNA expression in cardiac tissues. CircRes 1999;85(1):e1–e6.

6. Difrancesco D, Borer JS. The funny current: cellular basis for the control of heart rate. Drugs 2007;67:15–24. [PubMed: 17999560]

7. Bogdanov KY, Maltsev VA, Vinogradova TM, Lyashkov AE, Spurgeon HA, Stern MD, et al. Membrane potential fluctuations resulting from submembrane Ca2+ releases in rabbit sinoatrial nodal cells impart an exponential phase to the late diastolic depolarization that controls their chronotropic state. CircRes 2006;99(9):979–87.

8. Bogdanov KY, Vinogradova TM, Lakatta EG. Sinoatrial nodal cell ryanodine receptor and Na(+)-Ca (2+) exchanger: molecular partners in pacemaker regulation. CircRes 2001;88(12):1254–8.

9. Maltsev VA, Lakatta EG. Normal heart rhythm is initiated and regulated by an intracellular calcium clock within pacemaker cells. Heart Lung Circ 2007;16(5):335–48. [PubMed: 17827062]

10. Vinogradova TM, Lyashkov AE, Zhu W, Ruknudin AM, Sirenko S, Yang D, et al. High basal protein kinase A-dependent phosphorylation drives rhythmic internal Ca2+ store oscillations and spontaneous beating of cardiac pacemaker cells. CircRes 2006;98(4):505–14.

11. Joung B, Tang L, Maruyama M, Han S, Chen Z, Stucky M, et al. Intracellular calcium dynamics and acceleration of sinus rhythm by beta-adrenergic stimulation. Circulation 2009;119(6):788–96. [PubMed: 19188501]

12. Wu Y, Gao Z, Chen B, Koval OM, Singh MV, Guan X, et al. Calmodulin kinase II is required for fight or flight sinoatrial node physiology. ProcNatlAcadSciUSA 2009;106(14):5972–7.

13. Yeh YH, Burstein B, Qi XY, Sakabe M, Chartier D, Comtois P, et al. Funny current downregulation and sinus node dysfunction associated with atrial tachyarrhythmia: a molecular basis for tachycardia-bradycardia syndrome. Circulation 2009;119(12):1576–85. [PubMed: 19289641]

14. Mangoni ME, Nargeot J. Properties of the hyperpolarization-activated current (I(f)) in isolated mouse sino-atrial cells. CardiovascRes 2001;52(1):51–64.

15. Chen B, Wu Y, Mohler PJ, Anderson ME, Song LS. Local control of Ca2+-induced Ca2+ release in mouse sinoatrial node cells. J Mol Cell Cardiol 2009 Nov;47(5):706–15. [PubMed: 19615376]

16. Vinogradova TM, Bogdanov KY, Lakatta EG. beta-Adrenergic stimulation modulates ryanodine receptor Ca(2+) release during diastolic depolarization to accelerate pacemaker activity in rabbit sinoatrial nodal cells. CircRes 2002;90(1):73–9.

17. Le Scouarnec S, Bhasin N, Vieyres C, Hund TJ, Cunha SR, Koval O, et al. Dysfunction in ankyrin-B-dependent ion channel and transporter targeting causes human sinus node disease. Proc Natl Acad Sci U S A 2008 Oct 7;105(40):15617–22. [PubMed: 18832177]

18. Kwong KF, Schuessler RB, Green KG, Laing JG, Beyer EC, Boineau JP, et al. Differential expression of gap junction proteins in the canine sinus node. CircRes 1998;82(5):604–12.

19. Verkerk AO, van Borren MM, Peters RJ, Broekhuis E, Lam KY, Coronel R, et al. Single cells isolated from human sinoatrial node: action potentials and numerical reconstruction of pacemaker current. ConfProcIEEE Eng MedBiolSoc 2007;2007:904–7.

20. Satoh H. Suppression of pacemaker activity by Ginkgo biloba extract and its main constituent, bilobalide in rat sino-atrial nodal cells. Life Sci 2005;78(1):67–73. [PubMed: 16182317]

21. Vinogradova TM, Sirenko S, Lyashkov AE, Younes A, Li Y, Zhu W, et al. Constitutive phosphodiesterase activity restricts spontaneous beating rate of cardiac pacemaker cells by suppressing local Ca2+ releases. CircRes 2008;102(7):761–9.

22. Barbuti A, Crespi A, Capilupo D, Mazzocchi N, Baruscotti M, Difrancesco D. Molecular composition and functional properties of f-channels in murine embryonic stem cell-derived pacemaker cells. J Mol Cell Cardiol 2009;46(3):343–51. [PubMed: 19135060]

23. Verkerk AO, Wilders R, van Borren MM, Peters RJ, Broekhuis E, Lam K, et al. Pacemaker current (I(f)) in the human sinoatrial node. EurHeart J 2007;28(20):2472–8.

24. Wilders R, Verheijck EE, Kumar R, Goolsby WN, van Ginneken AC, Joyner RW, et al. Model clamp and its application to synchronization of rabbit sinoatrial node cells. AmJPhysiol 1996;271(5 Pt 2):H2168–H82.

25. Bucchi A, Baruscotti M, Robinson RB, DiFrancesco D. Modulation of rate by autonomic agonists in SAN cells involves changes in diastolic depolarization and the pacemaker current. J Mol Cell Cardiol 2007 Jul;43(1):39–48. [PubMed: 17543331]

26. Lakatta EG, Maltsev VA, Bogdanov KY, Stern MD, Vinogradova TM. Cyclic variation of intracellular calcium: a critical factor for cardiac pacemaker cell dominance. CircRes 2003;92 (3):e45–e50.

27. Lancaster MK, Jones SA, Harrison SM, Boyett MR. Intracellular Ca2+ and pacemaking within the rabbit sinoatrial node: heterogeneity of role and control. JPhysiol 2004;556(Pt 2):481–94. [PubMed: 14724216]

28. Platzer J, Engel J, Schrott-Fischer A, Stephan K, Bova S, Chen H, et al. Congenital deafness and sinoatrial node dysfunction in mice lacking class D L-type Ca2+ channels. Cell 2000 Jul 7;102(1): 89–97. [PubMed: 10929716]

29. Baruscotti M, Bucchi A, Difrancesco D. Physiology and pharmacology of the cardiac pacemaker ("funny") current. PharmacolTher 2005;107(1):59–79.

30. Liu J, Noble PJ, Xiao G, Abdelrahman M, Dobrzynski H, Boyett MR, et al. Role of pacemaking current in cardiac nodes: insights from a comparative study of sinoatrial node and atrioventricular node. ProgBiophysMolBiol 2008;96(1-3):294–304.

31. Baruscotti M, Barbuti A, Bucchi A. The cardiac pacemaker current. J Mol Cell Cardiol. 2009

32. Denyer JC, Brown HF. Pacemaking in rabbit isolated sino-atrial node cells during Cs+ block of the hyperpolarization-activated current if. JPhysiol 1990;429:401–9. [PubMed: 2177505]

33. Nof E, Luria D, Brass D, Marek D, Lahat H, Reznik-Wolf H, et al. Point mutation in the HCN4 cardiac ion channel pore affecting synthesis, trafficking, and functional expression is associated with familial asymptomatic sinus bradycardia. Circulation 2007;116(5):463–70. [PubMed: 17646576]

34. Schulze-Bahr E, Neu A, Friederich P, Kaupp UB, Breithardt G, Pongs O, et al. Pacemaker channel dysfunction in a patient with sinus node disease. JClinInvest 2003;111(10):1537–45.

35. Bucchi A, Baruscotti M, Robinson RB, DiFrancesco D. I(f)-dependent modulation of pacemaker rate mediated by cAMP in the presence of ryanodine in rabbit sino-atrial node cells. J Mol Cell Cardiol 2003 Aug;35(8):905–13. [PubMed: 12878477]
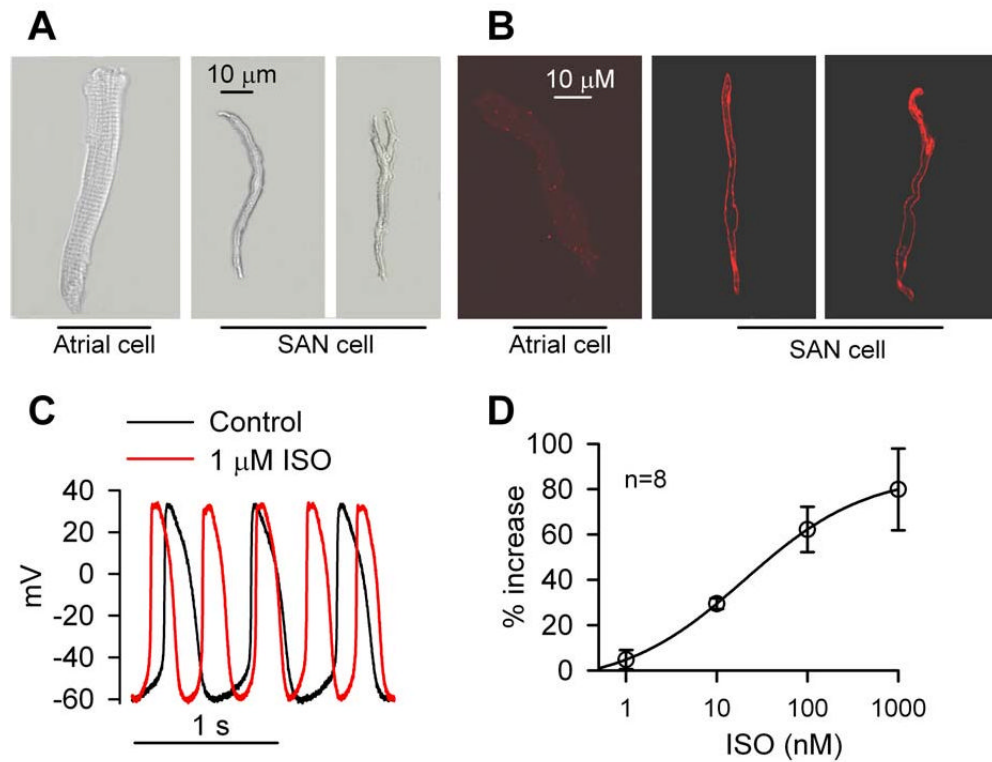
Fig 1.
Typical features of isolated dog SAN cells. **(A)** Typical morphology of isolated atrial and SAN cells. **(B)** SAN cells showed prominent HCN_4 staining, seen as green fluorescence, compared to atrial cells. **(C)** Representative action potential (AP) traces recorded before and after 1 μM isoproterenol (ISO). **(D)** ISO dose-dependently increased SAN cell AP frequency. The solid line shows the ISO – AP frequency relationship results fit with the Hill equation.
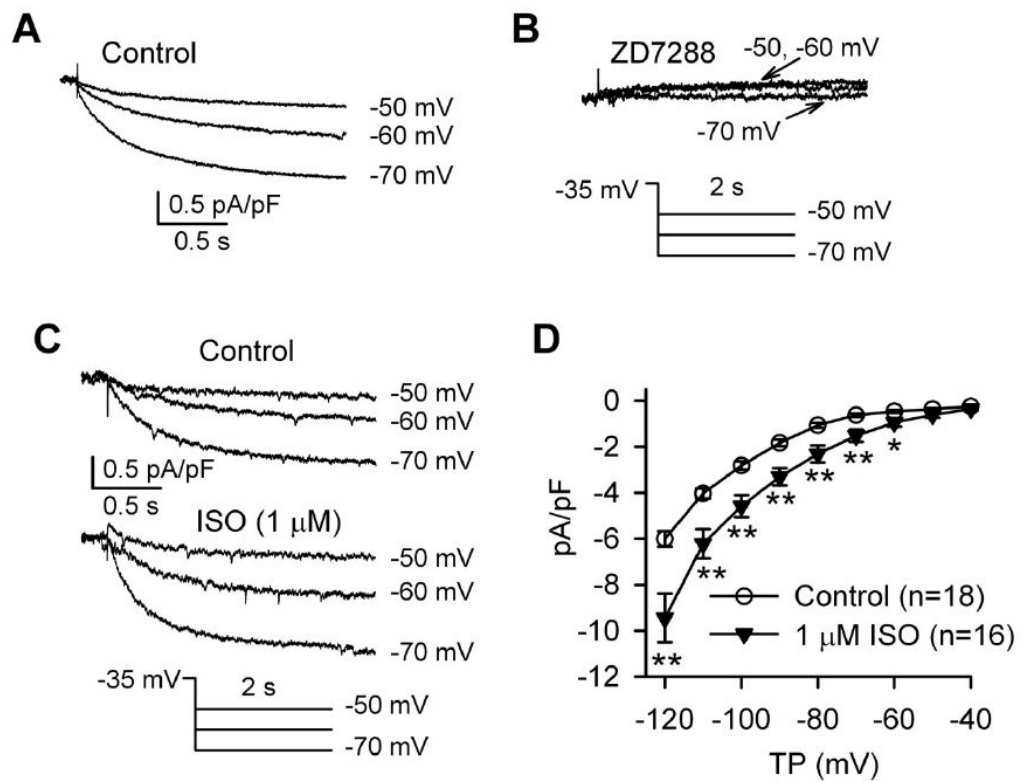
Fig 2.
ZD7288 and isoproterenol (ISO) effects on I_f. **(A)** Representative I_f traces recorded from an isolated canine SAN cell under control conditions and **(B)** in the presence of 3 μM ZD7288. **(C)** Representative I_f traces before and after ISO. **(D)** Current voltage (I-V) relationship of I_f under control conditions and in the presence of 1 μM ISO. *P<0.05 vs control; **P<0.01 vs control.
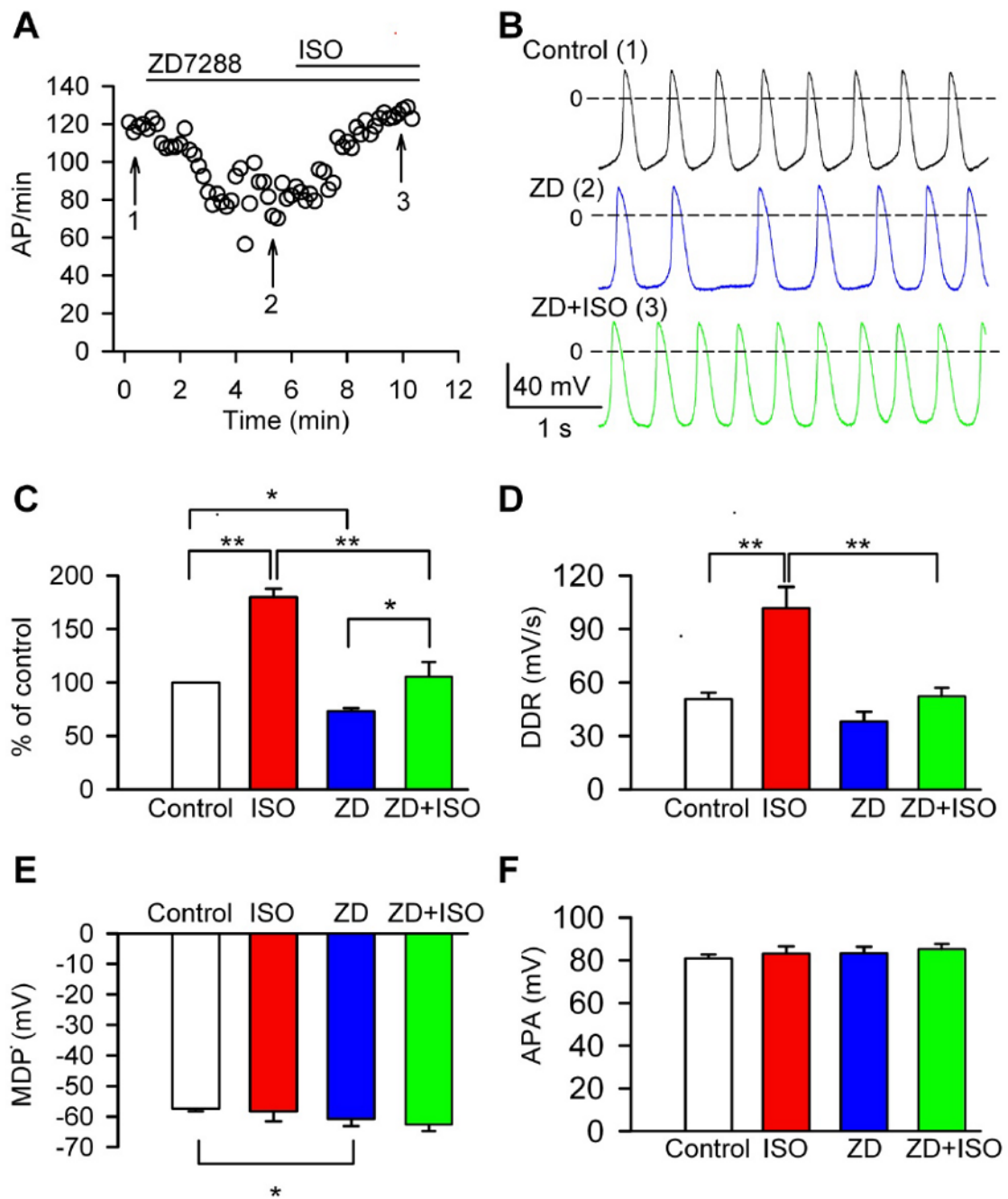
Fig 3.
ZD7288 reduced basal automaticity, caused arrhythmia and blunted rate acceleration by ISO. **(A)** Time course of pacemaker activity recorded in a typical SAN cell perfused sequentially with ZD7288 and the combination of ZD7288 and ISO. **(B)** AP traces recorded at the corresponding time points indicated by numerals in panel A. **(C)** Normalized pacemaker acitivity in control (n=21), in the presence of ISO (n=8), 3 μM ZD7288 (n=13), the combination of ZD7288 and ISO (n=6). *P<0.05, **P<0.01. **(D)** Summary data for diastolic depolarization rate (DDR) from cells in panel C. **P<0.01. **(E)** Summary data for maximum diastolic potential (MDP) from cells in panel C. *P<0.05 vs control. **(F)** Summary data for action potential amplitude (APA) from cells in panel C.
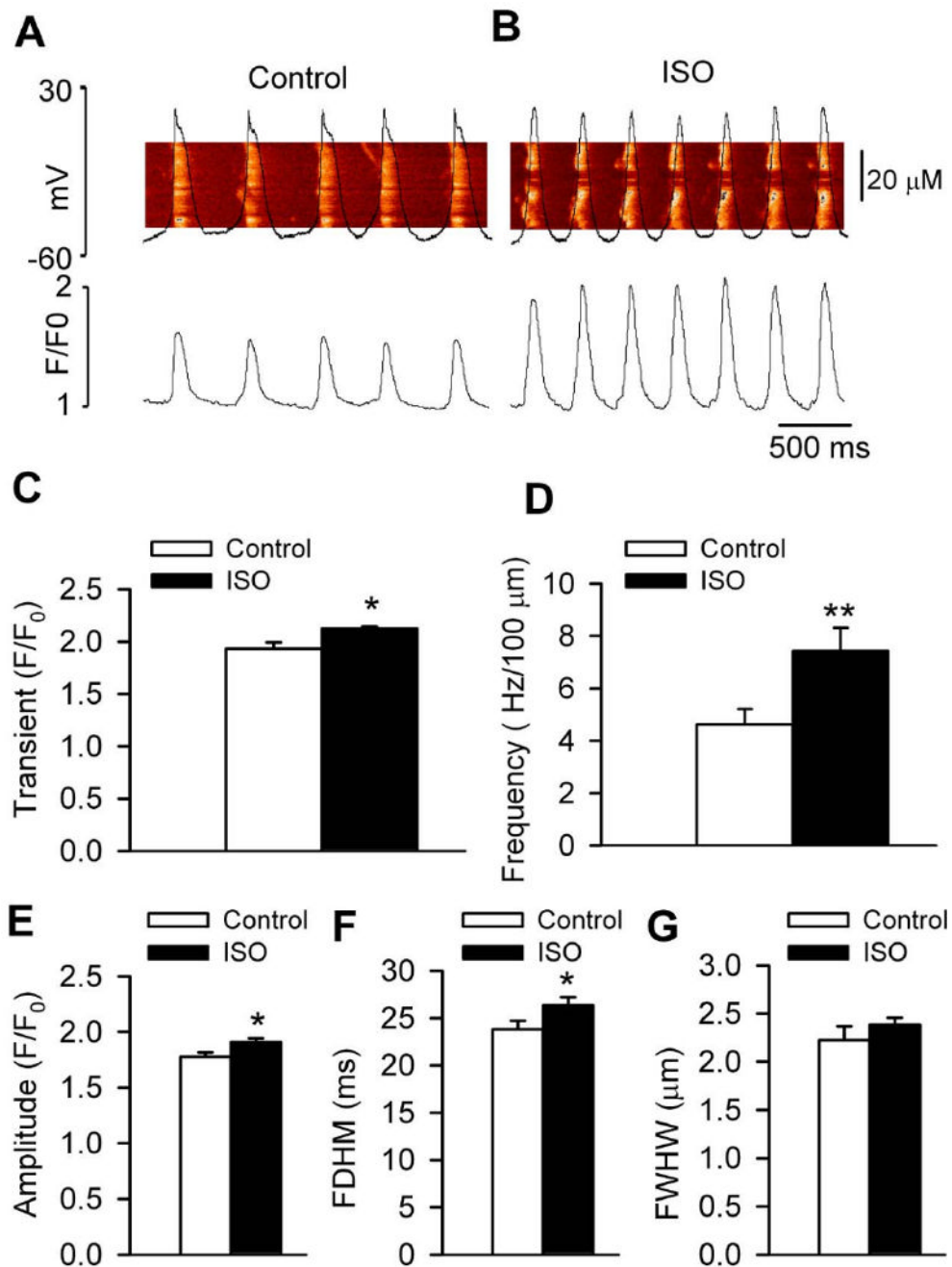
Fig 4.
ISO significantly enhanced the SR Ca^{2+} release in canine SAN cells. **(A-B)** Representative line scan confocal images of fluo 4 fluorescence and APs under control conditions **(A)** and during perfusion of 1 μM ISO **(B)**. **(C-G)** Summary data for Ca^{2+} transients (P=0.021) **(C)**, Ca^{2+} spark frequency (P=0.007) **(D)**, Ca^{2+} spark amplitude (P=0.015) **(E)**, Ca^{2+} spark duration (full duration at half-maximum, FDHM, P=0.045) **(F)**, Ca^{2+} spark width (full width at half-maximum, FWHM, P=0.262) **(G)**, before and after ISO (1 μM) (n=58–59 cells per group). *P<0.05 **P<0.01 vs control.
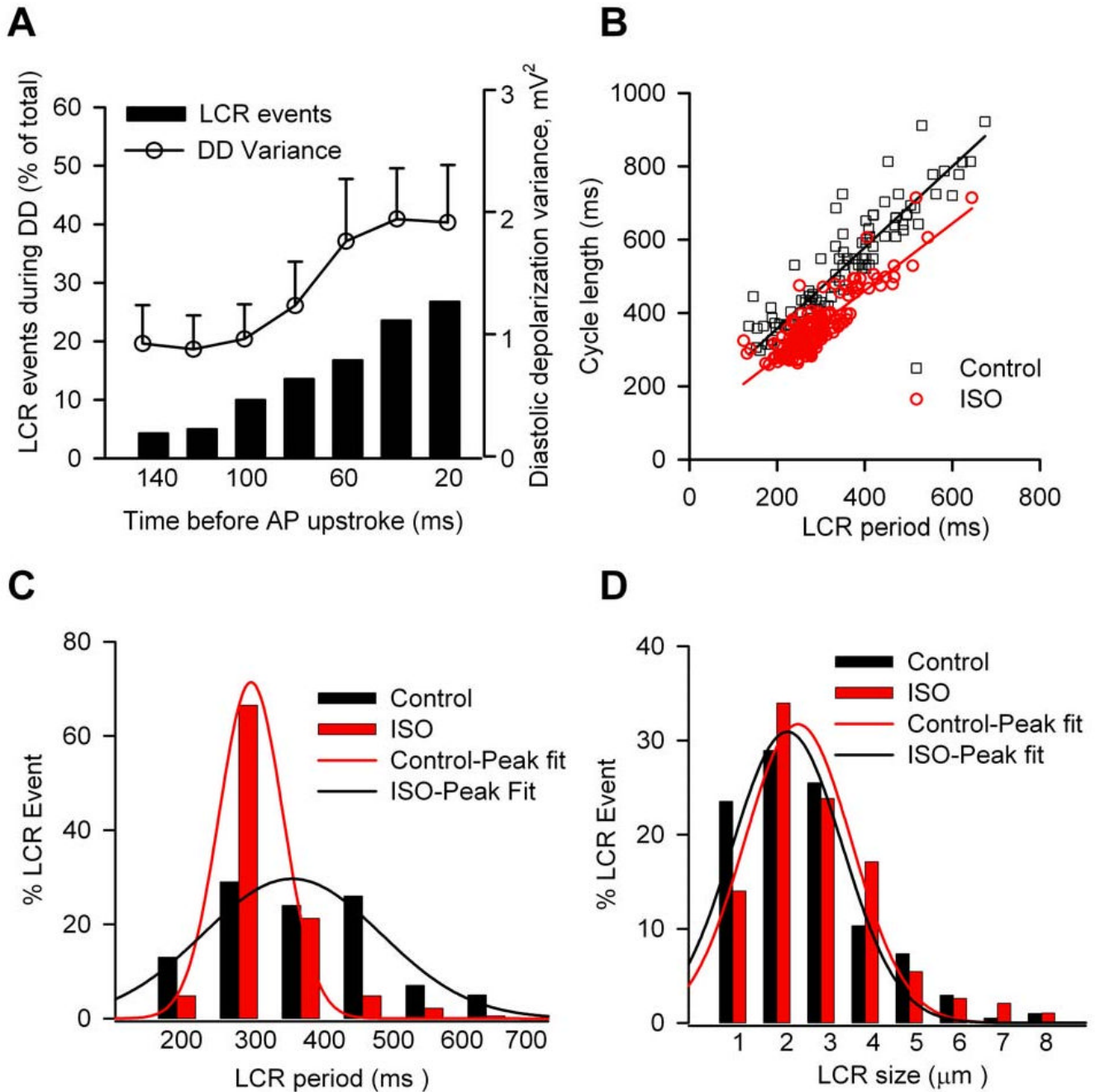
Fig 5.
Characteristics of local Ca^{2+} release (LCR) in dog SAN cells. **(A)** Time course of DD variance and of the relative LCR occurences observed at the different times before AP upstroke under control conditions. **(B)** Relationship between LCR period and spontaneous cycle length was shifted to shorter periods by 1 μM isoproterenol. **(C and D)** Proportional distribution of LCR period and size in control and at the presence of 1 μM isoproterenol. (n=58–59 cells per group)
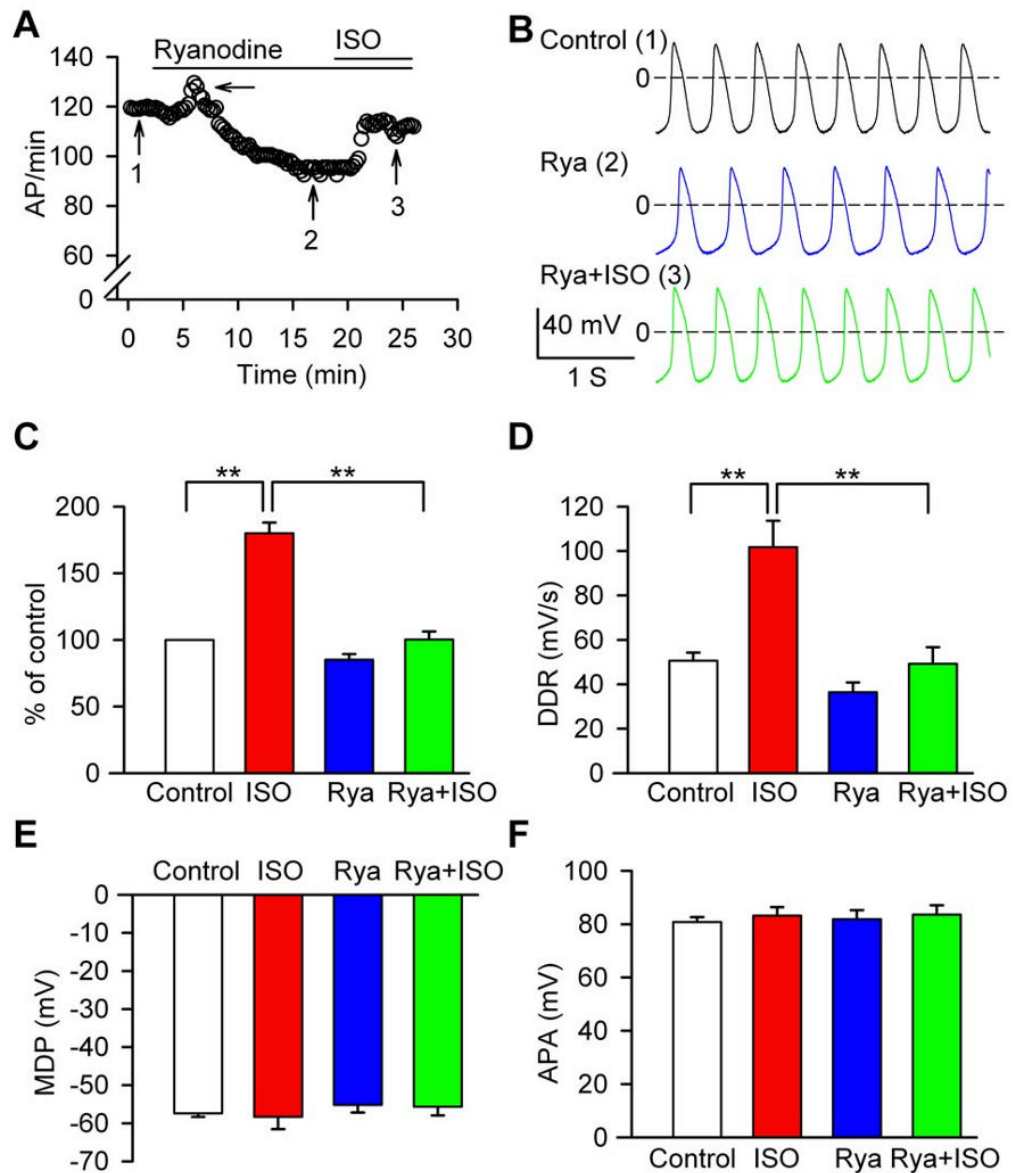
Fig 6.
Ryanodine effects on basal and ISO-stimulated APs. **(A)** Time course of pacemaker activity recorded in a typical cell sequentially perfused with 2 μM ryanodine and the combination of 1 μM ISO plus ryanodine. The arrow marks an increase in SAN cell automaticity at the initial phase of ryanodine treatment. **(B)** AP traces recorded at the corresponding time points indicated by numerals in panel A. **(C)** Normalized pacemaker activity in control (n=19), ISO alone (n=8), 2 μM ryanodine (n=11), and the combination of ryanodine plus 1 μM ISO (n=6). **P<0.01. **(D)** Summary data for DDR, **P<0.01. **(E)** Summary data for MDP. **(F)** Summary data for APA. Data in panels D-F are from cells in panel C.
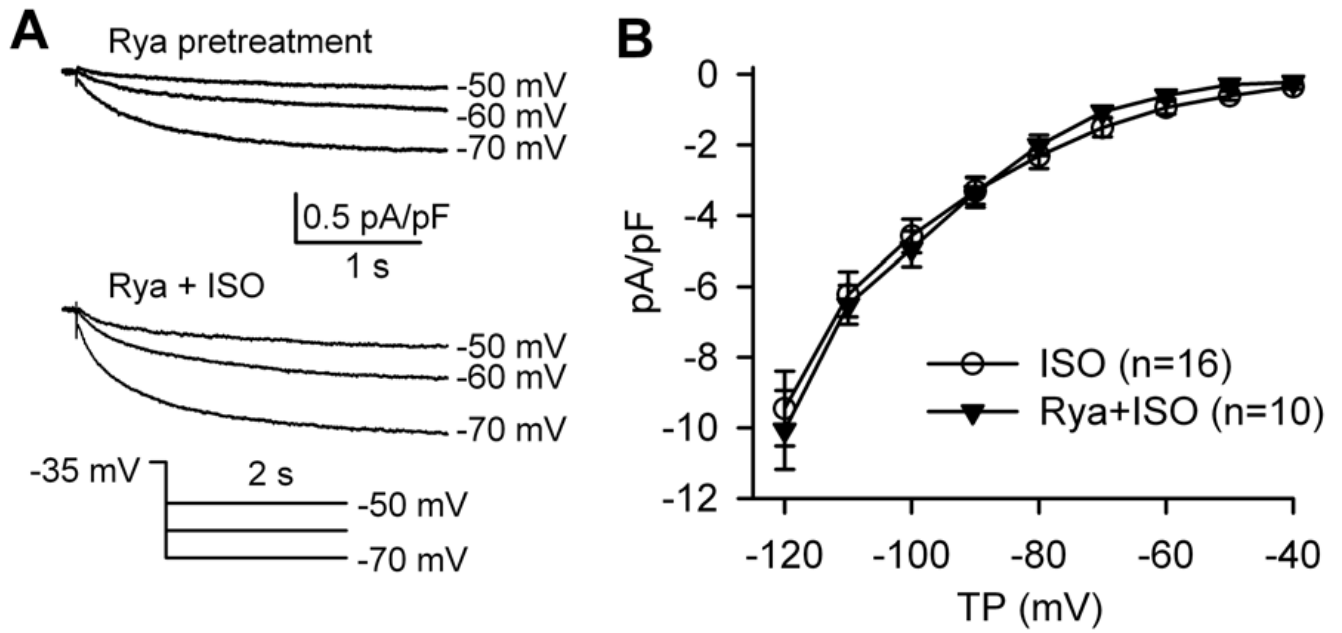
Fig 7.
Lack of effect of ryanodine on basal and ISO-treated I_f. **(A)** I_f traces in a typical SAN cell before and after ISO with ryanodine pretreatment. **(B)** I-V relationship of I_f in the presence of ISO with or without ryanodine pretreatment.